Original Research Article

Shoe Compression is Associated with Lower High-Frequency Spectral Power during Drop Landings: An Exploratory Analysis of Six Shoe–Wearer Conditions

Taylor A. Mangoba

Manlius Pebble Hill School, 5300 Jamesville Road, DeWitt, NY 13214, United States

ABSTRACT

Time-domain measures of landing impact may fail to capture information in the signal's frequency spectrum. Four female high-school students performed bilateral drop landings barefoot and while wearing six athletic shoes. For each landing, power spectral density estimates were derived from vertical ground reaction force recordings as well as tibial and sacral accelerometry. The within-participant deviation from barefoot landing was then correlated with the shoe's peak compression. The relationship was evaluated by frequency and then aggregated into three bands whose boundaries follow the running literature: 0–8 Hz (the movement component), 8–20 Hz (the impact component) and 20–100 Hz (above the impact component). Increased compression was associated with less absolute 20–100 Hz spectral power at the force plate ($r = -0.83$, leave-one-out [−0.96, −0.77]) and at the sacrum ($r = -0.96$, [−0.99, −0.88]). The bracketed ranges are the smallest and largest coefficients obtained when each shoe–wearer condition is left out in turn; hence they convey sensitivity and are explicitly not confidence intervals. Movement band power had a positive association with compression, although the force plate coefficient for this band approached zero with the removal of a single wearer-shoe pair. Furthermore, the coefficient for force plate total power reversed sign under leave-one-out, and the two non-saturated sensors yielded opposing directional relationships within the impact band. The most consistent association was a negative association between footwear compression and within-subject changes in 20–100 Hz spectral power. Since absolute 20–100 Hz power changes at the force plate and sacrum covaried closely across footwear conditions ($r \approx 0.8$), these two measurement sites appear to reflect a single underlying relationship rather than offering independent corroboration. All findings are exploratory given the small sample size and that each shoe was worn by only one person, so shoe and wearer cannot be separated, and the tibial signal was limited by ±16 g saturation.

Keywords: power spectral density; drop landings; biomechanics; compression testing; athletic shoes; ground reaction forces; accelerometers

INTRODUCTION

The musculoskeletal system is subjected to repeated contact with ground during activities such as running and jumping for sport. Several time domain measures have been identified to be associated with overuse injury, in particular tibial stress fractures. Female runners with a history of tibial stress fracture and those who go on

Corresponding author: Taylor A. Mangoba, E-mail: tmangoba@me.com.

Accepted August 25, 2026
https://doi.org/10.70251/HYJR2348.451931

to develop stress fractures of the tibia during running have been shown to have increased loading rates for vertical ground reaction force and higher peak tibial acceleration ('tibial shock') than controls of similar age and running experience (1). Interventions that decrease these measures are commonly used to try to prevent such injuries (2). However, there is only a weak correlation between time domain measures of ground reaction force and tibial shock, and the internal stress placed on the tibia during activity. It is believed that muscle contraction is the primary determinant of bone loading during activity, and that ground reaction force measures external loading of the tibia during activity (3). However, the frequency content of the impact may contain information not captured by peak values. This exploratory study examines if athletic shoe compression correlates with modifications in the spectral distribution of landing impacts.

The impact of a foot strike or landing generates a brief shock wave that travels upward through the body. Bones and soft tissue cause this physical wave to decline in intensity (4), alongside the movement of joints and the contraction of muscles (5, 6). The frequency composition of this wave might contain valuable data that are overlooked by focusing on maximum values in the time domain (7). Acceleration resulting from impacts on the lower extremities can be divided into two distinct categories. The first category is a low frequency element that reflects intentional bodily movements and the shifting of the center of mass. The second category is a high frequency element that reflects the rapid slowing down of the leg and foot when contact is made with the surface. Researchers refer to these distinct elements as the active and impact components (8). For accelerations measured in the lower limbs, these frequencies generally fall within the ranges of 3 – 8 Hz and 9 – 20 Hz (7). Since various types of injuries might be linked to specific regions of this frequency range, mapping out the distribution of impact energy and observing how shoes alter this distribution could provide greater insights than focusing on a solitary peak measurement.

Whether footwear cushioning reduces impact is contested. Although cushioning is intended to lower impact, softer and more heavily cushioned midsoles frequently produce equal or greater impact peaks and loading rates, apparently because the wearer increases leg stiffness in anticipation of a softer interface (9-11). Most of this evidence comes from running. The drop landing is a sharp deceleration task widely used in injury-risk screening (12), governed by similar mechanics, and a shorter, sharper deceleration transient carries its power at correspondingly higher frequencies (8). Frequency-domain analysis of footwear effects during landing is comparatively rare. This exploratory analysis therefore characterizes the spectral distribution of drop landing impacts at the force plate, tibia, and sacrum, and relates the within-participant change in that distribution to a mechanical measure of shoe cushioning, asking where in the spectrum shoe compression is associated with a change in spectral power.

METHODS AND MATERIALS

Participants and protocol

Four female high school students (A–D) participated. Inclusion criteria were enrollment in the author's high school class, age 16–17 years, regular participation throughout high school in an organized sport in which jumping is an important element, and voluntary interest in participating. The sole exclusion criterion, assessed by self-report, was any injury or other limitation posing elevated risk during repeated drop landings. No volunteer was excluded. Body mass ranged from 52 to 65 kg, height from 1.6 to 1.7 m, and US shoe size from 7 to 8.5. Participants performed bilateral drop landings from a 406 mm platform (effective drop height ≈356 mm). The drops were executed both barefoot and shod, stepping off without jumping, landing with one foot on each force plate, hands on hips, and stabilizing for at least two seconds before moving. Participants A and D each wore two pairs of shoes and B and C one pair of shoes, for six shoe-wearer observations (13). The study is an exploratory, non-randomized repeated-measures design in which each participant served as her own barefoot reference. The shoe-by-participant assignment is not complete, since no shoe was worn by more than one participant. Table 1 lists the ten participant-by-condition observations with their shoe characteristics, analyzed landings, and principal spectral outcomes.

The shoes are a subset of used athletic shoes characterized on a materials testing machine in a previous study (14), from which each shoe's peak compression (midsole displacement at 4,500 N) was taken; shoe numbers follow that analysis. Fit was that of everyday wear and no separate sizing or fitting procedure was applied (13). Each shoe was worn by only one participant, so shoe and wearer are confounded by design, and to emphasize this, the six conditions are referred to throughout as shoe–wearer conditions. Shoe order was not randomized; conditions were tested

Table 1. The ten participant-by-condition observations. *Peak compression (midsole displacement at 4,500 N), mid-load secant stiffness K_{mid} (secant slope of the loading curve from 1,000 to 2,500 N), and energy-return efficiency η are left–right pair means from the mechanical characterization of these shoes [13, 14]; barefoot rows have no shoe values. n is the number of matched drops analyzed per condition. The two spectral columns are condition means of per-drop absolute 20–100 Hz band power at the force plate and sacrum, computed as described in Methods. The outcome analyzed in the text is the within-participant change, each shod condition minus the same participant's barefoot condition, correlated with peak compression across the six shoe–wearer conditions. Values in parentheses beneath the spectral entries are the corresponding total 0–100 Hz band powers, which underlie the total-power correlations reported in the text.*

Participant	Condition	Peak compression at 4,500 N (mm)	K_{mid} (N/mm)	η (%)	n	Force plate 20–100 Hz (total 0–100 Hz) power (N²)	Sacrum 20–100 Hz (total 0–100 Hz) power (g²)
A	Barefoot	—	—	—	5	5,752 (170,635)	0.093 (0.819)
A	Shoe #4	23.4	303	52.5	4	9,851 (196,629)	0.121 (1.781)
A	Shoe #8	28.9	195	57.6	5	4,806 (182,390)	0.049 (0.759)
B	Barefoot	—	—	—	5	5,551 (127,175)	0.109 (1.074)
B	Shoe #9	29.5	190	53.4	6	3,065 (100,088)	0.113 (1.105)
C	Barefoot	—	—	—	4	8,098 (333,365)	0.177 (2.281)
C	Shoe #1	18.2	353	40.9	4	9,553 (268,644)	0.332 (2.122)
D	Barefoot	—	—	—	7	17,112 (213,086)	0.988 (3.658)
D	Shoe #13	33.4	176	55.8	4	7,023 (195,071)	0.844 (4.101)
D	Shoe #11	32.2	154	49.9	4	7,542 (232,797)	0.904 (5.870)

barefoot first, then each shoe. The drop landing data are from a companion study focused on time-domain outcomes (13). This paper reports a distinct frequency-domain analysis. The students were recruited from the author's high school class. Drops within a condition were self-paced, separated by the stabilizing time and the time needed to remount the platform. No structured rest periods were imposed. No practice or familiarization drops were performed before recording.

Shoe compression measurements

Peak compression values were taken unchanged from the prior characterization of these shoes (14). In that characterization, each shoe was compressed on an electromechanical materials-testing machine (Instron 5969, Instron, Norwood, MA) in a single symmetric load–unload cycle at 600 mm/min to a peak of 4,500 N, with the load applied through a 76 mm steel ball seated in the heel cup so that it was concentrated on the heel cushion; therefore, peak compression is the midsole displacement at the 4,500 N peak (13, 14). The left and right shoes of each pair were tested once each and their values averaged, treating the pair as the unit of analysis. Repeat tests of the same shoe were not performed, so within-shoe repeatability was not estimated. Since all six shoes were tested under the identical single-cycle protocol, protocol-dependent bias is shared across shoes, and therefore does not affect the between-shoe ordering of compression values. The 4,500 N load, relative to the landings analyzed here, is a high-load reference. The mean per-foot peak forces ranged from approximately 900 to 2,400 N and the largest condition-mean bilateral force was approximately 4,300 N (13). Since each shoe is loaded by one foot, the test load exceeds the largest observed per-foot landing load by roughly a factor of two. Peak compression at 4,500 N is therefore a standardized descriptor of each shoe's full compression curve rather than the displacement reached during these landings. In this six-shoe set it covaries closely with the other whole-curve descriptors ($|r| \geq 0.9$ with mid-load stiffness, absorbed energy, and shoulder-point displacement (13)), so associations with it should be read as associations with the shoe's overall compression behavior rather than with the displacement at any particular load.

Force plates and sensors

Vertical ground reaction force was recorded by dual force plates (PS-2142, PASCO Scientific, Roseville, CA) at 500 Hz. Resultant accelerations of the left and right tibia and of the sacrum were recorded by three skin-mounted triaxial accelerometers (MMS+ MetaMotionS, ±16 g per axis; Mbientlab, San Francisco, CA) at a nominal 400 Hz. Sensors were secured with shin guard sleeves and prewrap at the tibiae and a light brace at the sacrum. To quantify the extent of tibial saturation, the raw per-axis recordings of the 48 analyzed drops were examined. Within the −100 to +500 ms analysis windows, at least one tibial axis was at its ±16 g recording limit in all 96 limb-records (both limbs of all 48 drops), during the landing transient, with 379 saturated samples in total and a median of 4 per limb-record (range 1–10; approximately 12 ms at the ≈3 ms native sampling interval). The sacral axes never reached the 16 g limit on any axis within any analysis window (largest excursion 15.4 g, in one barefoot landing of participant D), so the analyzed sacral data contain no saturated samples.

Because the accelerometers deliver samples at irregular intervals (1–3 ms, median 3 ms), each accelerometer recording was resampled before spectral estimation onto a uniform 500 Hz grid spanning −0.5 to +2.0 s about each landing, identically for every participant and condition. Resampling used piecewise linear interpolation: the resultant acceleration was computed from the three axes at the native sample times, and that single series was then interpolated onto the uniform grid, rather than interpolating each axis and taking the resultant afterwards. Because the same interpolation was applied to every record, any smoothing it introduces is common to all conditions. Force plate records were already sampled uniformly at 500 Hz and were not resampled.

Gravity, static offsets, and sensor orientation were not removed before the resultant was computed. The sensors provide no orientation reference during the impact, so the gravitational component cannot be separated axis-wise, and the resultant accordingly rests at approximately 1 g before the landing (pre-landing medians in these data: sacrum ≈1.0 g, tibia ≈1.1–1.3 g including any calibration offset). The constant part of each windowed resultant, gravity included, was removed by the linear detrending applied before spectral estimation. Because the vector magnitude is a nonlinear operation, it can move some spectral content across frequencies, most plausibly into the low-frequency range while acceleration is small relative to 1 g. During the landing transient the resultant is dominated by accelerations many times gravity and the effect is second order. This processing is identical across conditions, but it is an additional reason the low-frequency accelerometer findings are treated as secondary and the interpretation is anchored on the force plate, which involves no magnitude operation.

The analysis was restricted to 0–100 Hz, below half the nominal sampling rate of both recording systems. Each landing was anchored to the first sustained crossing (three consecutive samples) of 200 N by the combined vertical force from both force plates, and the analysis window ran from −100 to +500 ms about that anchor, identical for every landing and channel.

Samples

A drop was counted as successful only if both force plates registered a peak above 100 N within ±0.2 s of the simultaneous left-plus-right peak (13). The force plates did not reliably sustain 500 Hz recording for a full session, and landings that consequently registered on one plate only were excluded, leaving four to seven force-plate drops per condition; the accelerometers recorded continuously and captured more landings than the force plates, five to twelve per condition (13). Because the accelerometers recorded continuously, their record constitutes the complete count of executed drops: 75 in total across the ten conditions. Of these, 27 were excluded, all for the instrumental reasons above rather than for any performance fault, leaving 48 retained drops. Per condition (executed / excluded / retained), the counts were 5/0/5, 6/2/4, and 7/2/5 for participant A (barefoot, #4, #8); 8/3/5 and 6/0/6 for participant B (barefoot, #9); 7/3/4 and 8/4/4 for participant C (barefoot, #1); and 7/0/7, 9/5/4, and 12/8/4 for participant D (barefoot, #13, #11) (13). Because the two instrument sets therefore covered different, though overlapping, drops, the present analysis was restricted to the landings in which all five locations (both force plates, both tibiae, and the sacrum) recorded the same drop, so that every sensor reflects the same landings. Every retained force-plate drop was also captured by all three accelerometers, so the matched set coincides with the retained force-plate drops. This yielded 48 matched drops, four to seven per condition.

Spectral analysis

Each windowed signal was linearly detrended and Hann-tapered. Its power spectral density was then computed as a periodogram with density scaling, so force spectra are in N^2/Hz and acceleration spectra in g^2/Hz. The computation used Welch's routine with a single segment covering the whole 600 ms window. With one segment nothing is averaged, so "Welch" refers only to the software routine used. The window is too short to split into segments without losing low-frequency resolution. Variance is reduced instead by averaging the spectra of individual drops within each condition. Because the spectra are densities, integrating over a frequency band gives the signal power in that band, in N^2 or g^2, and these powers are comparable across records sampled at different rates.

Each spectrum was then placed on a common frequency axis by linear interpolation: a 0.25 Hz grid from 0 to 100 Hz (401 points). The grid is only a shared axis and does not add resolution. The 600 ms window sets the true spacing of independent frequency points near 1.7 Hz, and the Hann taper roughly doubles that. Each interpolated value is a weighted average of its two neighboring true points, so nearby grid points are not independent. For this reason, the correlation spectrum (Statistics) is smooth below the true resolution, cannot contain independent features narrower than about 2–3.5 Hz, and is read only for broad patterns across frequency, never for single grid points.

For normalized quantities, each drop's spectrum was divided by its own total area over 0–100 Hz before averaging within its condition. Three bands are used throughout: 0–8 Hz (the active or movement component), 8–20 Hz (the impact component), and 20–100 Hz (all analyzed content above the impact component). The 8 and 20 Hz edges follow the running literature (7). Both edges fall exactly on grid points, and under the trapezoidal rule each edge point contributes half its weight to each of the two bands it borders. The three band powers therefore sum exactly to the 0–100 Hz total, with no frequency counted twice or left out. "Spectral power" is used in the signal-processing sense; the quantity is not mechanical energy, so "impact energy" is avoided. The force plate signal was the summed left-plus-right vertical force. Tibial spectra were computed for each limb and averaged. The sacrum used a single midline sensor.

Statistics

The unit of analysis throughout is the shoe–wearer condition, and the sample size for every correlation is $n = 6$. These six observations are not mutually independent: participants A and D each contributed two conditions, and each such pair shares both a wearer and that wearer's barefoot baseline, so the six points carry less information than six independent observations would. For this reason, and because the shoe-by-participant assignment is incomplete, no sampling-based inference is attempted, and no p-values or confidence intervals are attached to any coefficient. The Pearson correlation is used solely as a descriptive summary of the direction and approximate strength of linear association in this sample, and interpretation is restricted throughout to the sign of a coefficient and its stability under the leave-one-out procedures described below. For each sensor, at every frequency on the analysis grid, the Pearson correlation was computed across the six shoe–wearer conditions between the shoe's peak compression at 4,500 N (14) and the within-participant change (shod minus that participant's barefoot landing) in area-normalized power at that frequency. Plotting this coefficient against frequency yields a continuous correlation spectrum. To show which parts are stable rather than driven by a single shoe–wearer condition, a leave-one-out envelope was overlaid: omitting one shoe–wearer condition at a time yields six spectra, and the envelope spans their minimum and maximum at each frequency. The bracketed ranges reported alongside band-level coefficients are the analogous minimum and maximum across the six omissions; hence, they are descriptive sensitivity summaries, not confidence intervals. An envelope consisting entirely of positive correlations or entirely of negative correlations indicates that the sign of the association does not depend on any single shoe–wearer condition. Because participants A and D each contributed two shoe–wearer conditions, omitting one condition at a time cannot show whether a result depends on one participant. The band correlations were therefore repeated, omitting all of a participant's conditions at once. These are reported descriptively: with four or five observations the coefficients are not usable as estimates of effect size, and only the consistency of their sign is considered. Retention of the same sign under these omissions is a descriptive property of this dataset and is not intended to suggest statistical robustness, particularly because only five observations remain after each omission and some conditions are clustered within participants. Because adjacent frequencies are highly dependent, this is a descriptive display rather than a set of per-frequency tests. Again, since each shoe was worn by a single participant, these are exploratory associations, and they cannot separate the effect of the shoe from the effect of the person wearing it. Subtracting each participant's barefoot baseline removes that participant's overall level but not between-participant differences.

Absolute power analysis

Because area-normalized shares are compositional, a change in one band is arithmetically a change in the others, so the analysis was repeated using unnormalized spectra to establish which bands moved in absolute terms. For each landing, the unnormalized power spectral density was integrated over each of the three bands and over the full 0–100 Hz analysis range. For each shoe–wearer condition, the condition mean minus the same participant's barefoot mean was calculated and correlated with shoe peak compression using the same Pearson correlation and leave-one-out procedure described above. "Total power" refers to power integrated over 0–100 Hz. Throughout, "normalized power share" denotes a band's percentage of total power, "absolute band power" denotes the unnormalized power integrated over a band, and the "correlation spectrum" denotes the frequency-by-frequency correlation defined under Statistics; these are distinct quantities and are named consistently below. The Pearson correlation between the force plate and sacral changes was also calculated in absolute 20–100 Hz power across the six shoe–wearer conditions.

Window-taper sensitivity

For each landing, the analysis anchor was the first sustained crossing of 200 N by the combined vertical force from both force plates. This anchor occurred 100 ms after the start of the 600-ms analysis window, at approximately 17% of its duration, where the Hann taper had a weight of approximately 0.25 relative to its maximum at the window center. Actual contact onset, defined by the separate 30 N threshold used in the companion time-domain analysis, occurred slightly earlier and therefore received an equal or smaller Hann weight. To test whether this temporal down-weighting affected the force plate and sacral 20–100 Hz associations, the analysis was repeated using a Tukey window ($\alpha = 0.25$), for which the 200 N anchor lies within the flat central region. The analysis was also repeated with reduced tapering, including a Tukey window with $\alpha = 0.1$ and an untapered rectangular window. For each window, the compression correlations and leave-one-out ranges were recalculated using the same procedure described above. Supplementary Note S1 and Figure S1 illustrate the tapering step within a summary of the full analysis process.

Software

All analyses were performed in Python 3.12.3 with NumPy 2.4.4, SciPy 1.17.1, and openpyxl 3.1.5. Piecewise linear interpolation, both for the accelerometer resampling and for placing each spectrum on the common frequency grid, used numpy.interp. Detrending subtracted an ordinary least-squares line fitted with numpy.polyfit and evaluated with numpy.polyval. The Hann and Tukey tapers were generated with numpy.hanning and scipy.signal.windows.tukey. Power spectral densities were computed with scipy.signal.welch with the segment length set to the full window and density scaling. Band powers were integrated by the trapezoidal rule with numpy.trapezoid, and Pearson correlations were computed with numpy.corrcoef.

Ethical Considerations

This study was reviewed and approved by an institutional ethics review committee at Manlius Pebble Hill School, DeWitt, NY, composed of a faculty research advisor, the Dean of Academics, and the school nurse, whose membership provided health oversight; the committee judged the protocol minimal risk. No approval or reference number was assigned by the committee. Written parental or guardian permission and student assent were obtained before data collection, and the study was conducted in accordance with the principles of the Declaration of Helsinki. No sensitive personally identifiable information was collected: participants are identified only by letter and shoes by number in all data and analyses, video recordings were framed to generally avoid capturing participants' faces, and all data and video are stored on a password-protected computer.

RESULTS

Spectral distribution by sensor

Across all participants (Figure 1), the force plate spectrum was dominated by the 0–8 Hz movement band, the sacral spectrum fell off steeply above ~20 Hz and the tibial spectrum was distributed more broadly across the bands. The bands are unequal in size. Averaged across conditions, the force plate carried 90% of its signal power below 8 Hz, 6% between 8 and 20 Hz, and 4% above 20 Hz, and the sacrum 62%, 25%, and 13% respectively.

Greater compression tracks lower high-frequency spectral power. Figure 2 shows, for all three sensors, the correlation across the six shoe–wearer conditions between shoe peak compression and the within-participant change in area-normalized power at each frequency. The overall pattern is a positive association below roughly 8 Hz and predominantly negative associations at higher frequencies, although the pattern is not uniform across sensors or across the entire frequency range. At the force plate it is broad and negative from about 6 Hz upward. At the sacrum it is concentrated at higher frequencies, becoming predominantly negative

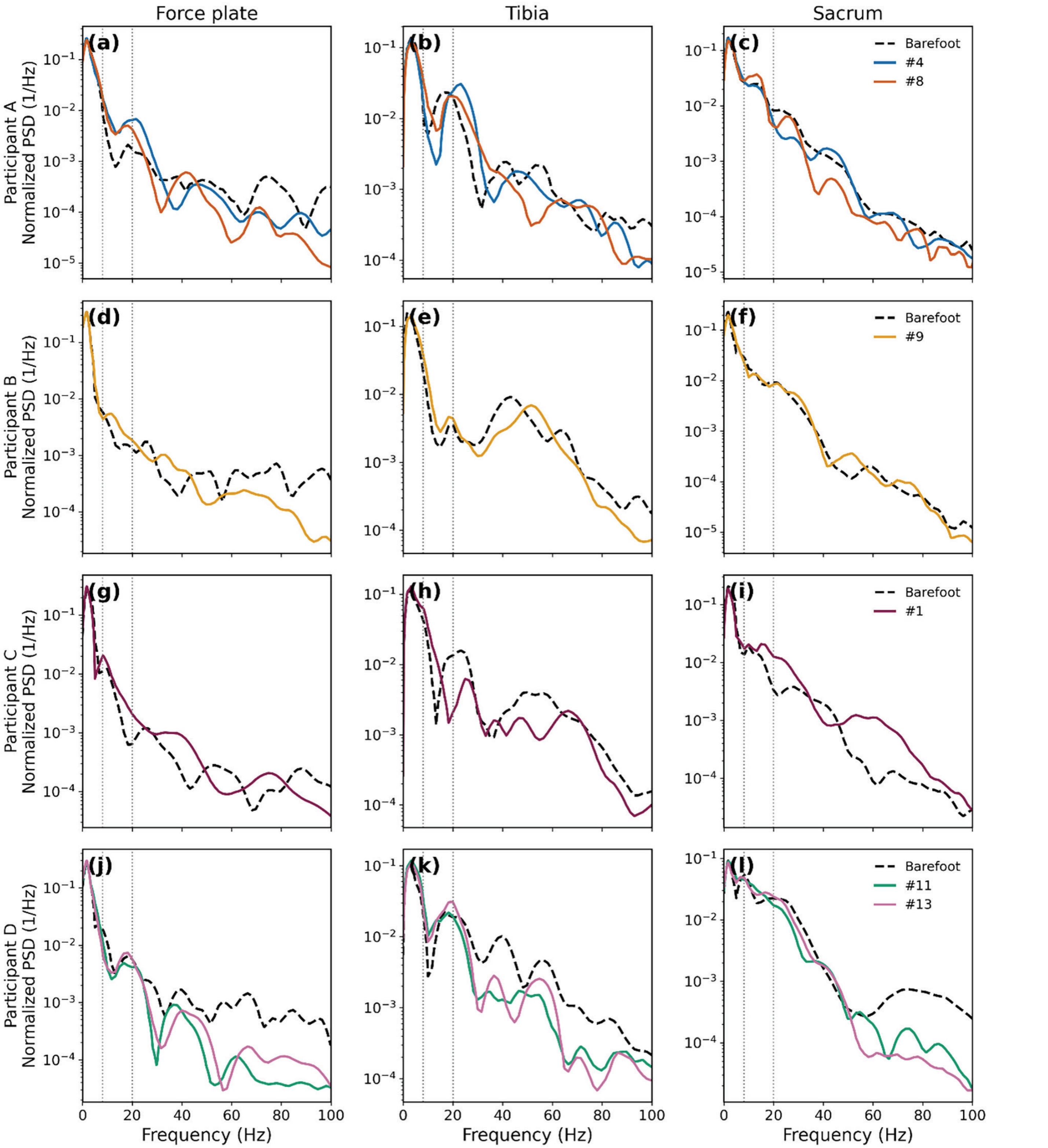

Figure 1. ***Power spectral density of drop landing impacts by participant (rows A–D).*** *Force plate is the summed left-plus-right vertical ground-reaction force; tibia is the left-plus-right average; sacrum is a single midline sensor. Each spectrum is area-normalized; log scale. Barefoot and each shoe–wearer condition (by shoe number) are overlaid.*

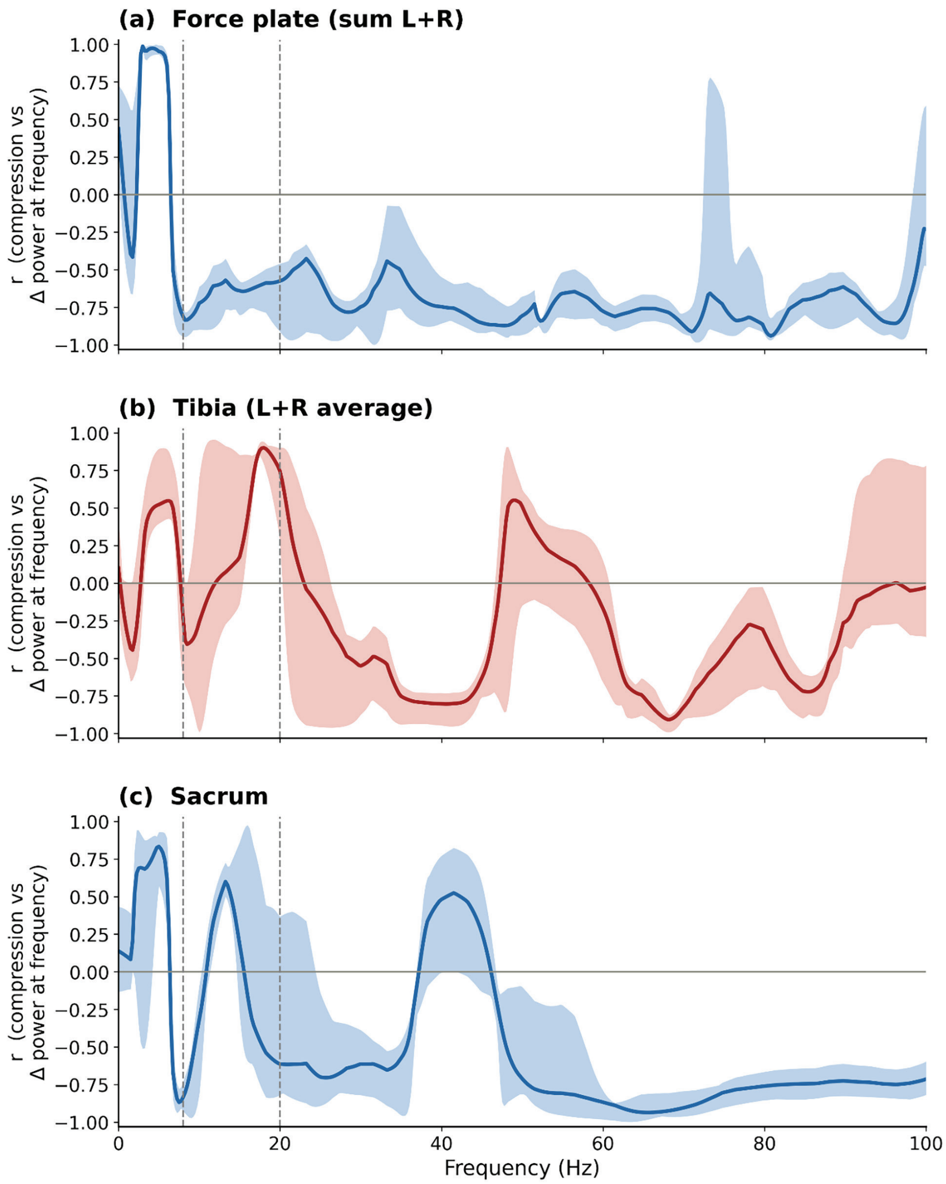

Figure 2. ***Continuous compression–spectrum association at all three sensors (exploratory; six shoe–wearer conditions).*** *For the force plate (a), averaged tibia (b), and sacrum (c), the solid line is the Pearson correlation across the six shoe–wearer conditions between shoe peak compression at 4,500 N and the within-participant change, relative to each participant's barefoot landing, in area-normalized power at each frequency. The shaded band is the leave-one-out envelope. Dashed lines delineate movement band and impact band.*

above about 20 Hz but showing a positive excursion between about 37 and 46 Hz. At the tibia the association is weaker and its envelope wide, consistent with ±16 g saturation degrading that channel. The leave-one-out envelope crossed zero in a few places, above about 72 Hz at the force plate and between about 20 and 46 Hz at the sacrum; hence the pointwise pattern was not uniformly sign consistent across the entire 20–100 Hz band. Because adjacent frequencies are highly dependent, no isolated frequency is interpreted as a separate finding. The band-level coefficients retained the same sign at both unsaturated sensors. A three-band summary in both normalized and absolute units is reported in Supplementary Tables S1 and S2.

Absolute-power analysis showed a similar directional association

The analysis was repeated in absolute (unnormalized) units. Greater compression was associated with lower absolute 20–100 Hz power at both unsaturated sensors (force plate r = −0.83, leave-one-out [−0.96, −0.77]; sacrum r = −0.96, [−0.99, −0.88]). Here and throughout, bracketed ranges are the minimum and maximum coefficients obtained when one shoe–wearer condition is omitted at a time; they are descriptive sensitivity summaries, not confidence intervals. Retention of the same sign across these omissions is a property of this sample: with five observations remaining after each omission, and with participants A and D each contributing two conditions, sign retention does not establish statistical robustness. Table 1 reports the condition-level band powers and analyzed landings underlying these correlations. Within that band the association was present in both halves, at 20–50 Hz (force plate −0.84, sacrum −0.91) and 50–100 Hz (−0.78 and −0.87). The force plate and sacral changes in absolute 20–100 Hz power were correlated across conditions (r ≈ 0.8). The other two bands were less consistent. The absolute movement-band (0–8 Hz) power rose with compression (force plate r = +0.68, leave-one-out [+0.02, +0.86]; sacrum +0.50, [+0.05, +0.69]), as did total 0–100 Hz power (+0.45, [−0.50, +0.77]; +0.39, [+0.10, +0.51]). However, omitting shoe #1 alone reduced the force plate movement-band coefficient to +0.02 and reversed the sign of the force plate total-power coefficient. In the impact band the two unsaturated sensors disagreed in sign (force plate −0.62, sacrum +0.38).

The force plate and sacral 20–100 Hz associations were not materially affected by the choice of window taper. With a Tukey window (α = 0.25), the correlations were r = −0.91 at the force plate, with a leave-one-out range of [−0.96, −0.89], and r = −0.87 at the sacrum, with a leave-one-out range of [−0.93, −0.66]. Across the additional taper choices, from a Tukey window with α = 0.1 to an untapered rectangular window, the force plate coefficient ranged from −0.91 to −0.93 and the sacral coefficient from −0.87 to −0.87. Both coefficients remained negative under every window tested. Omitting each participant in turn, rather than each condition, also left the 20–100 Hz association negative in every analysis at both unsaturated locations. For absolute band power the force plate coefficient was −0.91, −0.85, −0.96 and −0.68 when participants A, B, C and D respectively were omitted, against −0.83 for the full sample, and the sacral coefficient was −0.97, −0.99, −0.88 and −0.93, against −0.96. The normalized-share coefficients were negative throughout as well (force plate −0.80 to −0.95; sacrum −0.35 to −0.88). The other two bands were less consistent in sign under the same procedure. Absolute movement-band power remained positive in all four analyses but fell to +0.02 at the force plate and +0.05 at the sacrum when participant C was omitted. The sacral impact-band coefficient changed sign, from +0.38 to −0.78, when participant D was omitted.

Figure 3 plots the six shoe–wearer observations underlying the two absolute-power correlations, labeled by participant and shoe. The condition-level values, total powers, and the number of drops contributing to each condition mean are listed in Table 1.

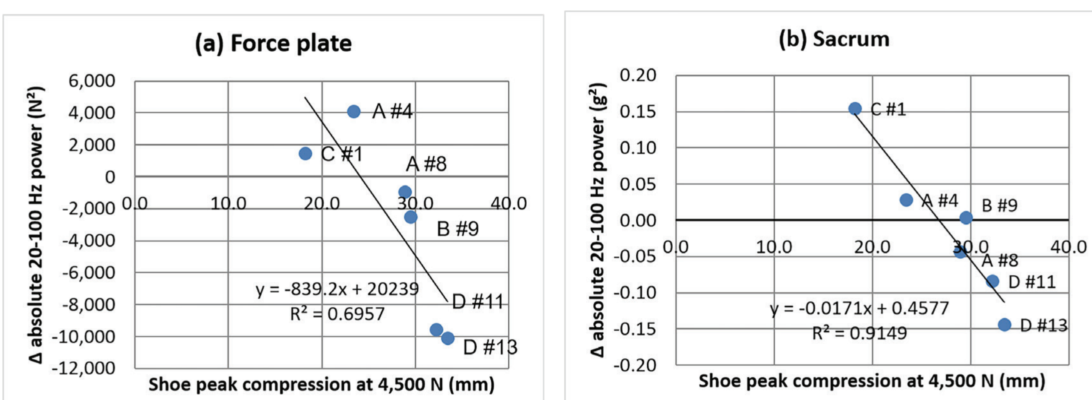

Figure 3. Absolute 20–100 Hz spectral power versus shoe peak compression, for the six shoe–wearer conditions. *Left panel, force plate; right panel, sacrum. The vertical axis is the within-wearer change in absolute 20–100 Hz power relative to that wearer's barefoot landing; the horizontal axis is the shoe's peak compression at 4,500 N. Each point is labeled by participant (A–D) and shoe number. Fitted lines are ordinary least squares fits shown for description only. Force plate r = −0.83 (leave-one-out [−0.96, −0.77]); sacrum r = −0.96 [−0.99, −0.88].*

DISCUSSION

The association whose direction was most consistently preserved across the sensitivity analyses, in both the normalized and the absolute analyses, was in the 20–100 Hz frequency range at the force plate and sacrum, relative to each wearer's barefoot baseline. The other bands were less consistent. Movement-band associations were positive at both unsaturated locations, but the force-plate coefficient fell nearly to zero when a single condition was omitted. Also, force-plate total power changed sign under leave-one-out while the sacral coefficient did not; and the two sensors disagreed in sign in the impact band. A noteworthy feature is that the association appears at the force plate, which is free of skin-mounting resonance and saturation, so the finding is not attributable to those accelerometer-specific artifacts. The force plate and sacral absolute 20–100 Hz power changes track each other across the six conditions, which indicates that the two sensors are describing largely one association at two levels of the body rather than providing two independent confirmations of it. Because each shoe was worn by only one participant, this association cannot be attributed to the footwear alone. Its direction was preserved in the reported sensitivity analyses, but its precision, its generalizability beyond these four participants, and its independence from participant characteristics remain unknown; the magnitude of the reported correlations should not be interpreted as evidence of a causal or participant-independent footwear effect.

In the area-normalized analysis, the association appeared as a change in normalized power share whose direction was most consistently preserved under omission, and whose coefficient was largest at high frequency. Compression was associated with a larger 0–8 Hz share and a smaller 8–100 Hz share at the force plate and sacrum. This normalized pattern should not be interpreted as an absolute transfer of power into the movement band. Total power moved with the movement band rather than remaining fixed, so the spectrum is not redistributing a conserved quantity. In the three-band summary the loss is concentrated above the impact component, and the association runs in the same direction but more weakly at the saturation-affected tibia (Table S1).

The association lay above the conventionally studied impact range, and the band was defined to make that boundary explicit. The running studies from which the band edges were adapted place the impact component nearer 9–20 Hz (7), while Shorten and Winslow (8) treated 60–100 Hz accelerometer content as susceptible to attachment resonance and judged that contamination to have little or no influence below 50 Hz. Frequency-domain analyses of running further report that tibia-to-head shock attenuation is concentrated at the impact frequencies and above them, with peak shank-to-head attenuation reported in the 15–50 Hz range (8), while components below roughly 6 Hz can show a gain rather than attenuation (7, 8). In vivo measurements during walking likewise show impact transients progressively attenuated as they travel up the skeleton, with the heel-strike wave itself carrying its major frequency component at 25–35 Hz (4). Even so, band power above 20 Hz has not been quantified in this literature: signal power has been reported only within 3–8 and 9–20 Hz ranges (7); attenuation analysis has been restricted to 10–20 Hz on the grounds that minimal head and tibial acceleration power existed above 20 Hz in running (15); and although Shorten and Winslow considered components up to 100 Hz, band power above 20 Hz was not quantified there either, and the 60–100 Hz portion was set aside as resonance-prone (8). That is a difference between tasks, not merely an analysis choice: a discrete bilateral drop landing is a shorter, sharper deceleration transient than a running foot strike, and within running, spectral peak frequencies scale with the inverse of contact time (8). Extending that principle across tasks, the shorter landing transient should carry its power at correspondingly higher frequencies, and in these data measurable force plate and sacral power did extend throughout 20–100 Hz (Table 1). The association reported here therefore sits above the range in which the running literature localizes the impact component, in content that was left unquantified or treated as artifact-prone. Running-derived band edges and findings should not be assumed to transfer unchanged to drop landings.

Reported natural frequencies for skin-mounted accelerometer systems vary substantially across studies, from roughly 27–41 Hz to 60–100 Hz (8, 15). This is a further reason to anchor the interpretation on the force plate result. The reduction was also present in the lower half of the band, 20–50 Hz, which lies below the 60–100 Hz range treated as resonance-susceptible (8), so attachment resonance is an unlikely sole explanation for it, although the lower reported estimates near 27–41 Hz do overlap this half of the band.

The higher-frequency location of the association is nevertheless plausible rather than anomalous, although this was not tested directly here. Several sources could in principle contribute power above 20 Hz, and they are not mutually exclusive: the contact transient itself, whose sharpness places genuine signal content at high frequency; transmission of that transient through the foot, footwear, and skeleton, which would carry biomechanical meaning; skin-mounted accelerometer attachment resonance, which affects the sacral channel but not the force plate; and instrumentation characteristics of the force plates themselves, such as structural resonance of the plate and its mounting, which were not characterized in this study. The present data cannot apportion the observed 20–100 Hz power among these sources, except that attachment resonance can be excluded at the force plate, which has no sensor-to-skin coupling. What can be concluded is that shoe compression was associated with the high-frequency content of the landing signal as measured externally; whether all of that content reflects biomechanically meaningful loading of internal structures cannot be determined from these data.

These findings should be read against the "cushioning paradox," in which softer or maximal shoes often fail to reduce, or even increase, impact-peak magnitude and loading rate during running (9–11). The present result is not in conflict with that literature. The cushioning-paradox studies concern time-domain summaries such as impact-peak magnitude and loading rate, whereas this result concerns the 20–100 Hz band of spectral power. These measures characterize different aspects of the landing signal and need not change in parallel.

A reasonable concern is that the resolvable part of the association sits at high frequency, where area-normalized power is smallest and where tibial saturation and sacral attachment resonance are concentrated. The most direct test addresses the normalization itself: in absolute units the reduction above the impact component persists and retains its sign under leave-one-out, so it is not an artifact of normalization. Absolute movement-band power was also positively associated with compression, but the force plate coefficient fell nearly to zero when one condition was omitted. The corresponding increase in normalized movement-band share may partly reflect the compositional complement of the reduction above the impact component. The most defensible reading is that greater compression was associated with lower spectral power above the impact component, and that the accompanying movement-band gain is too dependent on a single condition to be distinguished from the arithmetic complement of that reduction.

Referencing each condition to the same wearer's barefoot landing removes that wearer's overall level but does not separate the shoe from the person wearing it. Every association reported here is therefore an association across six shoe–wearer conditions.

Because external impact metrics are only weakly related to internal tibial bone load (3), the clinical meaning of a spectral shift remains uncertain and should not be over-interpreted. No spectral threshold of injury risk exists for landing, and no outcome data connect the 20–100 Hz band to injury, tissue loading, or performance. The association reported here establishes at most that shoe compression is related to a measurable property of the external landing signal; whether that property matters for internal loading, injury, or performance is unknown and cannot be inferred from these data.

Limitations

Each shoe was worn by only one participant, so shoe and participant effects cannot be separated; hence no analysis reported here can establish a footwear effect independent of the wearer. Participants A and D each contributed two shoe conditions, so the six observations are not fully independent, and the paired conditions share both a wearer and a barefoot baseline. A leave-one-participant-out sensitivity analysis was therefore run alongside the condition-level analysis (Results). Shoe order was not randomized, so order and fatigue effects cannot be ruled out. Barefoot landings were also always collected first, so any shod-versus-barefoot comparison is confounded with order, fatigue, and familiarization. Tibial spectra are compromised by ±16 g saturation, which distorts tibial power, so tibial results are reported as exploratory and potentially biased. For the same reason, the tibia-to-sacrum attenuation analysis was not pursued. The absolute tibial 20–100 Hz association is weak and not leave-one-out stable ($r = -0.18$); hence, no inference is drawn from it. The band boundaries are adapted from running studies. The spectral content of a discrete landing may differ, and the bands should be regarded as reasonable approximations rather than task-specific thresholds.

CONCLUSION

In this exploratory analysis of six shoe–wearer conditions, greater shoe compression was associated with a smaller normalized power share and lower absolute spectral band power in the 20–100 Hz band, above the conventionally defined impact component for running, at both the force plate and the sacrum relative to each participant's barefoot condition. Movement-band and total power associations were sensitive to single conditions, and no firm conclusion is drawn about them. Because each shoe was worn by only one participant, the result does not establish a causal footwear effect independent of the wearer. The finding characterizes the externally measured landing signal, and no outcome data connect this band to injury or performance. A larger randomized crossover study in which every participant wears every shoe, with unsaturated tibial sensors, is needed to separate footwear effects from participant differences.

Supplementary Note S1. Why the window taper was checked

A power spectrum is calculated from a finite segment of a signal. If the beginning and end of that segment do not match, treating the segment as a complete record creates an artificial jump at the boundary and spreads power across frequencies, a problem called spectral leakage. A taper reduces this problem by gradually lowering the signal toward zero at the edges of the segment. The main analysis used a Hann taper, which rises smoothly from zero, reaches full weight at the center of the window, and then falls back to zero.

Here, the landing occurred early in the 600-ms analysis window. The 200 N anchor occurred 100 ms after the window began, where the Hann taper had a weight of 0.25, and actual contact began slightly earlier. In the example shown in Figure S1, the Hann taper retained 60% of the barefoot force peak and 51% of the shod peak. The peaks occurred at different times relative to the anchor, +70 ms and +52 ms, and therefore fell at different points on the rising portion of the taper. If every record were attenuated by the same overall factor, the shod-minus-barefoot differences would be rescaled by that factor and their correlation with compression would be unchanged. Because the attenuation was not identical across records, it could alter the correlation, and this motivated the sensitivity analysis.

The analysis was therefore repeated using Tukey windows with $\alpha=0.25$ and $\alpha=0.1$, as well as an untapered rectangular window. With the Tukey $\alpha=0.25$ window, the example impact peaks fell within the flat central region and were not attenuated by the window. The resulting coefficients are reported in the Results. No conclusion in this paper depends on the choice of taper.

Supplementary Tables S1 and S2. Pearson correlation ($n = 6$ shoe–wearer conditions) between shoe peak compression at 4,500 N and the within-participant change from barefoot in each band. Each coefficient was recomputed six times, omitting one shoe–wearer condition each time; brackets give the smallest and largest of those six values, so a bracket that stays one side of zero indicates a sign that does not depend on any single condition. The three shares in Table S1 sum to 100%, so a gain in one band is necessarily a loss across the others, so the rows cannot be read as three separate tests. Table S1 is read alongside the continuous spectrum in Figure 2. Absolute band powers are not shares of a fixed total, so all three can rise together or fall together, and a reduction in Table S2 reflects less power in that band rather than a loss of share.

The bracket indicates whether the sign is preserved under omission. Its endpoints are the two most extreme of six values, each computed from five remaining conditions, and because the conditions are unevenly spread across the compression range a single high-leverage condition can move the coefficient substantially in either direction. Tibial coefficients are not independent of ±16 g saturation and are reported as an exploratory, potentially biased secondary analysis.

CONFLICT OF INTEREST

The author declares that there are no conflicts of interest related to this work.

AI DISCLOSURE STATEMENT

During the preparation of this work, the author used Claude for coding, editing and extending their understanding of power spectral decomposition. Following the use of this tool or service, the author carefully reviewed, verified, and edited the content as necessary and takes full responsibility for the accuracy, originality, and integrity of the published work.

REFERENCES

1. Milner CE, Ferber R, Pollard CD, Hamill J, Davis IS. Biomechanical factors associated with tibial stress fracture in female runners. *Med Sci Sports Exerc.* 2006; 38 (2): 323–328. https://doi.org/10.1249/01.mss.0000183477.75808.92
2. Crowell HP, Milner CE, Hamill J, Davis IS. Reducing impact loading during running with the use of real-time visual feedback. *J Orthop Sports Phys Ther.* 2010; 40 (4): 206–213. https://doi.org/10.2519/jospt.2010.3166
3. Matijevich ES, Branscombe LM, Scott LR, Zelik KE. Ground reaction force metrics are not strongly

correlated with tibial bone load when running across speeds and slopes: implications for science, sport and wearable tech. *PLoS ONE*. 2019; 14 (1): e0210000. https://doi.org/10.1371/journal.pone.0210000

4. Wosk J, Voloshin A. Wave attenuation in skeletons of young healthy persons. *J Biomech*. 1981; 14 (4): 261–267. https://doi.org/10.1016/0021-9290(81)90071-3
5. DeVita P, Skelly WA. Effect of landing stiffness on joint kinetics and energetics in the lower extremity. *Med Sci Sports Exerc.* 1992; 24 (1): 108–115. https://doi.org/10.1249/00005768-199201000-00018
6. Nigg BM, Mohr M, Nigg SR. Muscle tuning and preferred movement path — a paradigm shift. *Curr Issues Sport Sci.* 2017; 2: 007. https://doi.org/10.36950/CISS_2017.007
7. Gruber AH, Boyer KA, Derrick TR, Hamill J. Impact shock frequency components and attenuation in rearfoot and forefoot running. *J Sport Health Sci.* 2014; 3 (2): 113–121. https://doi.org/10.1016/j.jshs.2014.03.004
8. Shorten MR, Winslow DS. Spectral analysis of impact shock during running. *Int J Sport Biomech.* 1992; 8 (4): 288–304. https://doi.org/10.1123/ijsb.8.4.288
9. Clarke TE, Frederick EC, Cooper LB. Effects of shoe cushioning upon ground reaction forces in running. *Int J Sports Med.* 1983; 4 (4): 247–251. https://doi.org/10.1055/s-2008-1026043
10. Baltich J, Maurer C, Nigg BM. Increased vertical impact forces and altered running mechanics with softer midsole shoes. *PLoS ONE*. 2015; 10 (4): e0125196. https://doi.org/10.1371/journal.pone.0125196
11. Kulmala JP, Kosonen J, Nurminen J, Avela J. Running in highly cushioned shoes increases leg stiffness and amplifies impact loading. *Sci Rep.* 2018; 8: 17496. https://doi.org/10.1038/s41598-018-35980-6
12. Hewett TE, Myer GD, Ford KR, *et al*. Biomechanical measures of neuromuscular control and valgus loading of the knee predict anterior cruciate ligament injury risk in female athletes: a prospective study. *Am J Sports Med*. 2005; 33 (4): 492–501. https://doi.org/10.1177/0363546504269591
13. Mangoba TA. Exploratory associations between shoe compression mechanics and tibial and sacral shock during bilateral drop landings. Unpublished manuscript.
14. Mangoba TA. Testing the shoulder point compression framework on 13 pairs of used athletic shoes. *Am J Stud Res.* 2026; 4 (4): 169–182. https://doi.org/10.70251/HYJR2348.44169182
15. Mercer JA, DeVita P, Derrick TR, Bates BT. Individual effects of stride length and frequency on shock attenuation during running. *Med Sci Sports Exerc.* 2003; 35 (2): 307–313. https://doi.org/10.1249/01.MSS.0000048837.81430.E7

SUPPLEMENTARY FILES

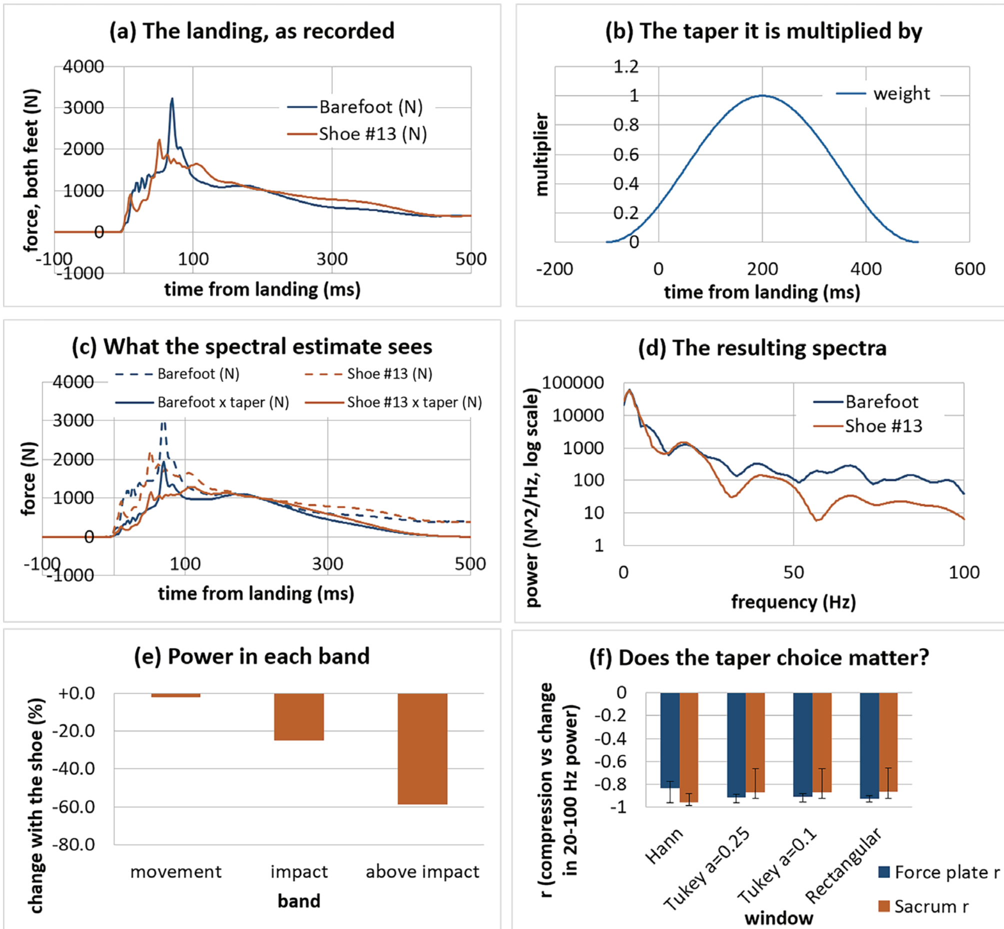

Figure S1. ***Six steps in the spectral-analysis pipeline, illustrated using participant D barefoot and shoe #13.*** *(a) Recorded vertical force. (b) The Hann taper; its weight at the 200 N anchor is 0.25. (c) Force signals before tapering (dashed) and after tapering (solid); the barefoot and shod peaks retain 60% and 51% of their original heights, respectively. (d) The resulting force plate spectra with the three analysis bands indicated. (e) Percentage change in unnormalized band power for this example condition relative to barefoot; this percentage display is illustrative, whereas the statistical analysis used unscaled shod-minus-barefoot differences. (f) The correlation between compression and the change in 20–100 Hz power under each window; bars show leave-one-out ranges, not confidence intervals. Panels (d) and (e) illustrate one condition; the associations across all six shoe–wearer conditions are reported in the main text.*

Table S1. Correlation with compression: change in each band's normalized power share (its area-normalized share of total power). *At each location, the three shares sum to 100% within each condition, so the three shod-minus-barefoot changes sum to zero and their signs are not independent. Because absolute band powers are not shares of a fixed total, all three can rise or fall together; a reduction in Table S2 is therefore a real reduction rather than a loss of share to another band.*

Band	Force plate	Tibia	Sacrum
0–8 Hz	+0.80 [+0.73, +0.92]	+0.30 [+0.01, +0.80]	+0.70 [−0.08, +0.96]
8–20 Hz	−0.74 [−0.89, −0.65]	+0.35 [+0.08, +0.95]	−0.22 [−0.56, +0.55]
20–100 Hz	−0.86 [−0.95, −0.81]	−0.34 [−0.93, −0.12]	−0.77 [−0.88, −0.35]

Table S2. Correlation with compression: shod minus barefoot change in absolute band power. *Additional rows report the same correlation for total 0–100 Hz power and for the 20–100 Hz band split at 50 Hz.*

Band	Force plate	Tibia	Sacrum
0–8 Hz	+0.68 [+0.02, +0.86]	+0.58 [+0.15, +0.77]	+0.50 [+0.05, +0.69]
8–20 Hz	−0.62 [−0.91, −0.49]	+0.69 [+0.58, +0.84]	+0.38 [+0.03, +0.48]
20–100 Hz	−0.83 [−0.96, −0.77]	−0.18 [−0.96, +0.27]	−0.96 [−0.99, −0.88]
Total (0–100 Hz)	+0.45 [−0.50, +0.77]	+0.54 [−0.17, +0.90]	+0.39 [+0.10, +0.51]
20–50 Hz	−0.84 [−1.00, −0.78]	−0.19 [−0.95, +0.30]	−0.91 [−0.95, −0.72]
50–100 Hz	−0.78 [−0.85, −0.69]	−0.09 [−0.68, +0.17]	−0.87 [−0.93, −0.82]